Two-dimensional, Viscous Flow Modeling of Roll-back Subduction: Numerical Investigation into the Role of Slab Density in Subduction Dynamics

by

Jessica L. Haurin

Submitted to the Department of Earth, Atmospheric and Planetary Sciences
in Partial Fulfillment of the Requirements for the Degree of
Bachelor of Science in Earth, Atmospheric and Planetary Sciences
at the Massachusetts Institute of Technology
September 10, 2004

Author Signature redacted
Department of Earth, Atmospheric and Planetary Sciences
September 10, 2004

Certified by Signature redacted
Dr. Leigh Royden
Thesis Supervisor

Accepted by Signature redacted
Dr. Samuel Bowring
Chair, Committee on Undergraduate Program

Two-dimensional, Viscous Flow Modeling of Roll-back Subduction:
Numerical Investigation into the Role of Slab Density in Subduction Dynamics

by

Jessica L. Haurin

Submitted to the Department of Earth, Atmospheric and Planetary Sciences

September 10, 2004

In Partial Fulfillment of the Requirements for the Degree of Bachelor of Science in Earth, Atmospheric and Planetary Sciences

ABSTRACT

Observations of retreating subduction systems in the Mediterranean region suggest the density of subducting lithosphere is dynamically related to trench retreat rate and upper-plate deformation. Most numerical and analog studies of retreating subduction systems have not explored the effects of lithospheric density variations on subduction processes. This study is a preliminary effort to construct a two-dimensional, viscous flow model of "roll-back" subduction to explicitly examine how slab density influences retreat rate, mantle flow, and slab geometry. For a given lithosphere-mantle density contrast, the model computes the evolution of a viscous, thermal slab using a finite element code for incompressible convection (ConMan). Imposed velocity boundary conditions guide lithospheric material into a uniformly weak "subduction zone" and out into the mantle below, generating stable, asymmetric subduction. Slabs driven faster than the "intrinsic" (dynamically consistent), steady-state retreat rate of the system (v_r) are characteristically arcuate, pushed upward from the base of the mantle layer by strong horizontal "return flow" beneath the descending lithosphere. Slabs driven slower than v_r are sigmoidal: the slabs steepen at depth, where vertical buoyancy forces overcome lateral viscous forces set up by weak surface velocities. The diagnostic behaviors of slabs driven faster and slower than v_r define a set of qualitative criteria (slab geometry, mantle flow patterns) for converging on the consistent, steady-state retreat rate of the system. For slab-mantle density contrast $\Delta\rho = 198$ kg/m^3 (defined as the density difference between lithosphere at surface of the system and mantle material at the base of the system), $v_r \approx 16$ mm/yr. The slab is roughly planar, with 50° dip. For $\Delta\rho = 168$ kg/m^3, v_r is slightly slower (14 mm/yr), and steady-state slab geometry is nearly identical (moderately-dipping planar surface). It is found that the angle at which lithospheric material is forced into the mantle does not significantly affect either steady-state retreat rate or slab geometry.

Thesis Supervisor: Dr. Leigh Royden, Professor of Geology and Geophysics

To haurin.1 and haurin.2,

who gave me M.I.T.

TABLE OF CONTENTS

INTRODUCTION

Subduction processes are intimately related to the system of global plate motions, but the dynamic relationships among plate motions, subducting lithosphere, and the mantle interior are not well known. Where subduction rate exceeds rate of overall plate convergence[1], subduction boundaries migrate ("retreat") away from the rigid interior of the overriding plate. Based on observations of retreating subduction systems in the Mediterranean region, Royden (1993b) suggested retreating boundaries develop during the early stages of continent-continent collision and consume oceanic lithosphere "trapped" between irregularly-shaped, converging landmasses. Moreover, Royden (1993a,b) and others (e.g. Le Pichon, 1982) have argued that gravitational "pull" on dense, oceanic lower-plate material is the principle driving mechanism for subduction along retreating boundaries (causing descending slabs to "roll-back" toward the interior of the downgoing plate).

Geophysical and geological surveys of the Mediterranean region document a strong correlation, both in space and time, between locations of actively retreating subduction systems and distribution of negatively buoyant lithosphere. This observational research compellingly, but qualitatively, links the density of downgoing lithosphere to retreat rate and thus to the dynamics of subduction.

Quantitative descriptions of the role of slab density in subduction processes are less well developed. Geodynamic modeling is a versatile and controlled approach to "quantifying" observed relationships between lithospheric density and subduction rate. Moreover, it is a technique for examining these relationships in terms of dynamic processes at depth. This study develops a preliminary numerical viscous flow model of roll-back subduction using a finite element code for two-dimensional, incompressible convection (ConMan). The model calculates the evolution of a viscous slab given prescribed surface velocities and/or stresses. Results are then evaluated for "dynamic self-consistency" (i.e. the question is asked: Does the chosen surface velocity artificially place net stress on the slab?) in order to converge on a consistent, steady-state retreat rate for the system. The study is designed to explore explicitly how slab

[1] After Royden (1993a), subduction rate is defined as the rate at which the subduction boundary (trench) moves relative to the rigid interior of the downgoing plate. Rate of overall plate convergence is defined as the relative rate of movement between the interior of the downgoing plate and the interior of the overriding plate.

density affects retreat rate and how interactions between descending lithosphere and surrounding mantle control slab geometry and mantle flow patterns.

The model presented here represents a "first step" in constructing a numerical simulation of density-driven subduction that can be tested against the behavior of natural systems (e.g. retreating subduction systems in the Mediterranean). The results of this study will guide development of a new generation of subduction models that are both more realistic (they should calculate rather than prescribe retreat rates) and more flexible (they should consider positively buoyant as well as negatively buoyant slabs). The end goal is to develop a dynamically self-consistent numerical model of roll-back subduction to quantitatively examine the effects of lithospheric density variations on trench retreat rate, slab morphology, surface deformation, and mantle flow and to determine the length and time scales on which these effects occur.

EVOLUTION OF RETREATING SUBDUCTING SYSTEMS: EVIDENCE FROM THE MEDITERRANEAN REGION

Royden and Burchfiel (1989) have suggested that systematic variations in the style and orientation of thrusting in the Mediterranean region are associated with regional tectonism along two distinct types of subduction boundaries (Fig. 1). In areas where the African-Arabian and Eurasian continents have collided (e.g. eastern Turkey), orogenic belts have formed in response to horizontal shortening across the plate margin. These belts typically trend perpendicular to the direction of plate convergence. Where the Mediterranean basin separates the two continents, upper-plate extension occurs behind arcuate, thin-skinned contractional belts (e.g. the Hellenic and Carpathian thrust systems) that are generally oriented obliquely to relative plate motions (reviewed in Royden, 1993b).

These two types of marginal thrust belts have diagnostic structural and morphological signatures that reflect fundamental differences in dynamic processes at depth. Upper-plate shortening is characteristic of "advancing" subduction systems, where rate of overall plate convergence exceeds rate of subduction, and the convergent boundary moves toward the rigid interior of the overriding plate (Fig. 2, left). Orogenic belts developed along advancing margins typically have high topography, undergo extensive erosion, and commonly contain high-grade metamorphic rocks exposed in basement-cored folds and thrusts. In contrast, upper-plate extension occurs where convergence rate is less than subduction rate, and the plate boundary migrates away from the interior of the overriding plate (Fig. 2, right). Thrust belts along these "retreating" boundaries generally have low topography, experience minor erosion, and predominantly involve low-grade to unmetamorphosed rocks (reviewed in Royden, 1993b). Over the past three decades, characterization of subduction boundaries in the Mediterranean region has provided an empirical basis for inferring the tectonic forces that drive these systems. Researchers have proposed several different (but perhaps complementary) dynamic models of Mediterranean tectonics.

McKenzie (1972) suggested retreating subduction systems in the Mediterranean basin lie along the margins of minor plates that developed in response to the collision of continental Eurasia and Arabia, near Iran. Positively buoyant continental material does not easily subduct.

Figure 1 Tectonic map of the Mediterranean region, showing motions of the major plates. Double barbed lines represent advancing plate margins; single barbed lines represent retreating plate margins; double-headed arrows show locations of regional extension. From Kahle *et al.* (1995).

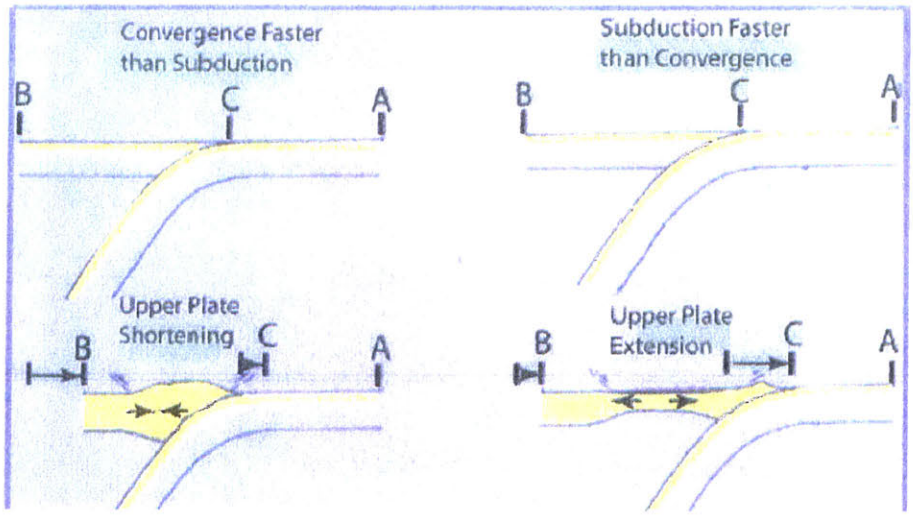

Figure 2 Diagram of the two types of subduction boundaries and associated styles of upper-plate deformation. Top row shows initial plate configuration. The change in the length of line AB represents convergence rate; change in the length of line AC represents subduction rate. Left column shows the evolution of an advancing subduction system (convergence rate exceeds subduction rate); right column shows the evolution of a retreating subduction system (convergence rate is less than subduction rate). From Royden *et al.* (2003).

Thus, McKenzie hypothesized that a dual process of crustal thickening beneath the collision zone and lateral extrusion of continental material out of the collision zone (rather than subduction) accommodates continued convergence across the Arabian-Eurasian margin. He argued that crustal flow directed away from the point of collision has initiated development of new plate boundaries that move obliquely to the direction of continental convergence (Fig. 3). These young, retreating subduction systems consume the dense oceanic floor of the Mediterranean basin until they stagnate against a continental margin and produce a new generation of microplates.

McKenzie's tectonic model of the Mediterranean region implies seaward migration of retreating subduction boundaries is a consequence of horizontal compressional stresses produced by lateral flow of continental material. Le Pichon (1982), however, argued that mature subduction processes in the Mediterranean basin operate largely independently of far-field stresses, effectively "self-driven" by the release of gravitational potential energy stored in negatively buoyant subducting lithosphere. He suggested that although horizontal stresses due to regional tectonics and lateral density changes across continental margins may be necessary for the initiation of subduction, once downwelling has sufficiently progressed, dense, downgoing lithosphere will exert a "slab-pull" force strong enough to continue subduction in its own right. As the subducting slab "rolls back" through the mantle under the force of gravity, the subduction

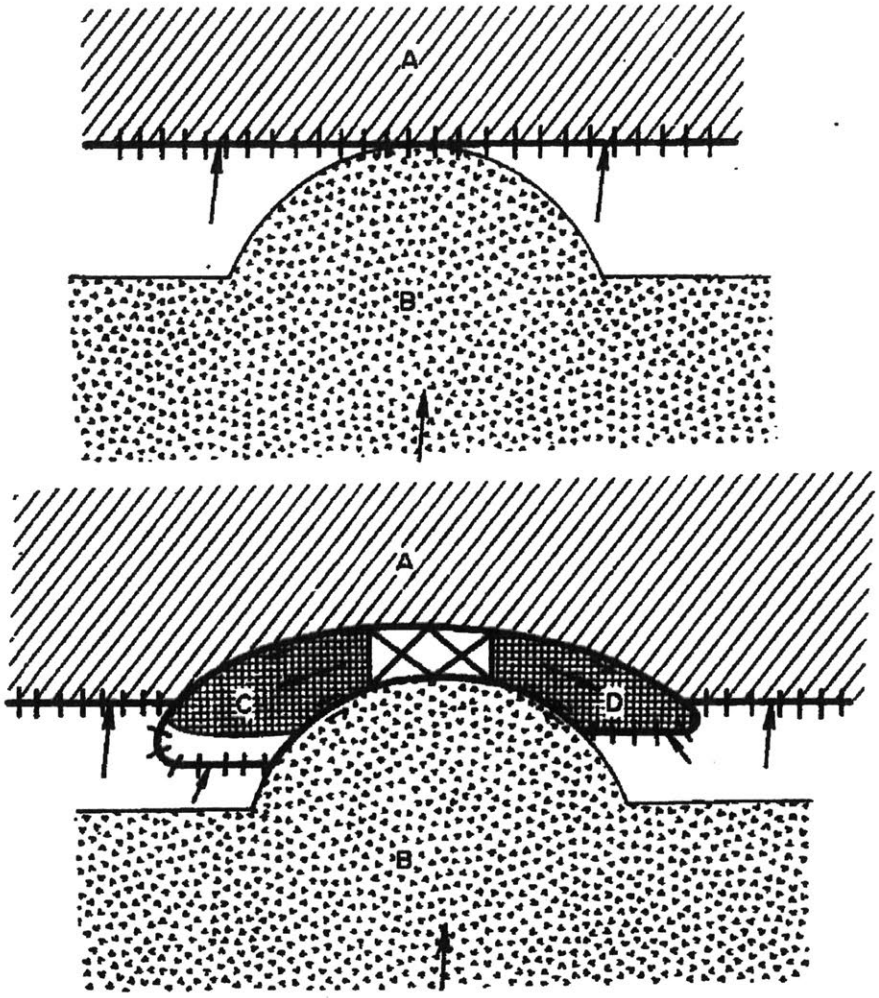

Figure 3 Schematic diagram of collision between two irregularly-shaped continental masses (A and B). Top: Plates A and B converge along a subduction boundary oriented perpendicular to the direction of relative plate motion. Where the two plates collide, positively buoyant continental material enters the trench, and subduction stagnates. Bottom: To accommodate postcollisional convergence, continental material extrudes laterally away from the collision zone, forming two new, smaller plates (C and D) that move obliquely to the direction of major plate convergence behind secondary retreating subduction boundaries. From McKenzie (1972).

boundary retreats oceanward, closing the deep-sea basin in the foreland and opening an extensional basin in the back-arc. It follows from Le Pichon's model that the lifespan of a retreating subduction system depends on the size and shape of the ocean basin available for consumption (Royden, 1993b).

Royden (1993b) synthesized McKenzie's and Le Pichon's mechanisms for trench retreat, developing a conceptual model of continent-continent collisional tectonics centered around a dynamic relationship between advancing and retreating subduction systems. She proposed that advancing plate boundaries develop along the margin where two irregularly-shaped, converging

continents first collide in order to accommodate postcollisional shortening. Like McKenzie, she suggested horizontal compressional stresses related to crustal thickening beneath the collision zone induces lateral flow of continental material away from the collision point behind secondary retreating subduction boundaries. Nevertheless, Royden pointed out that back-arc structures associated with retreating subduction systems are characteristically extensional rather than compressional. Thus, like Le Pichon, she reasoned slab pull must eventually become the major driving force for subduction.

SLAB DENSITY AND TRENCH MIGRATION: OBSERVATIONS FROM THE HELLENIC ARC

The Hellenic system is a young, retreating subduction boundary in the east-central Mediterranean region that has shown both spatial and temporal variability in the density of subducting lithosphere. The Hellenides thus provide an excellent observational setting in which to examine the relationships among slab density, subduction rate, and upper-plate deformation and the length and time scales on which these relationships operate.

The Hellenic arc extends southeastward for ~1000 km from the southern Adriatic Sea into the Ionian Sea, where it bends eastward south of Crete. Off the southwestern coast of mainland Greece, the northern and southern segments of the arc are dextrally offset by ~100 km along the southwest-trending Kephalonia Transform (Fig. 4). This transform represents a tectonic boundary across which the rate of subduction, style of deformation, and density of

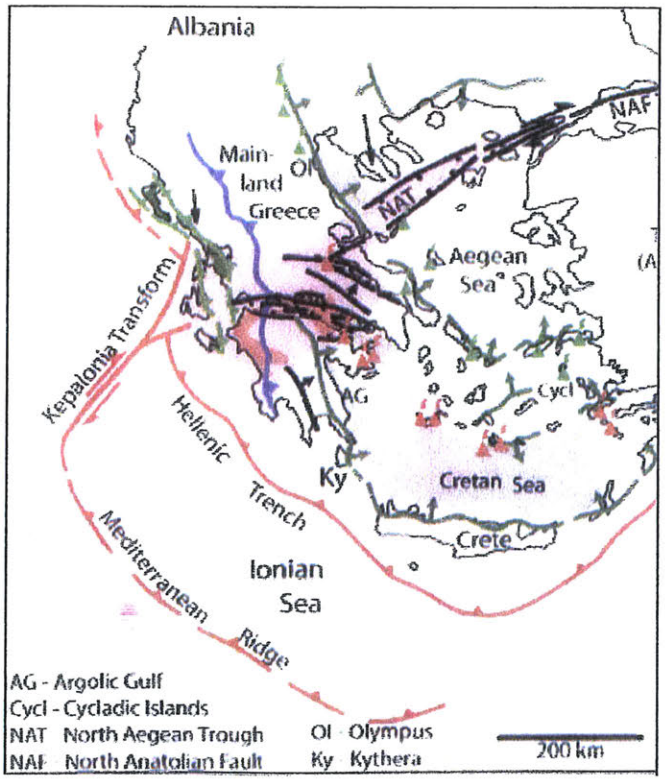

Figure 4 Map of the Hellenic subduction system in the east-central Mediterranean region. Solid red lines are the modern subduction boundaries; blue line is the continuous Pindos thrust front (late Eocene) in the external Hellenides; light pink shaded region is the Central Hellenic Shear Zone. From Royden *et al.* (2003).

downgoing lithosphere change, suggesting the geographic discontinuity in the Hellenic subduction boundary reflects a fundamental change in the nature of subduction at depth (reviewed in Royden *et. al.*, 2003).

Geodetic surveys of the Aegean region show that north of the Kephalonia Transform, the convergence rate across the Hellenic arc is ~10 mm/yr relative to southern Italy. Folding and thrusting along this northern portion of the Hellenides defines a narrow belt of contractional deformation. South of the transform, convergence occurs much more rapidly: ~40 mm/yr with respect to stable Eurasia. Here, the thrust belt broadens eastward more than 200 km to the Mediterranean Ridge. Within this belt, shortening involves only a thin sedimentary cover; the underlying basement is subducted at the trench (Fig 5; reviewed in Royden *et. al.*, 2003).

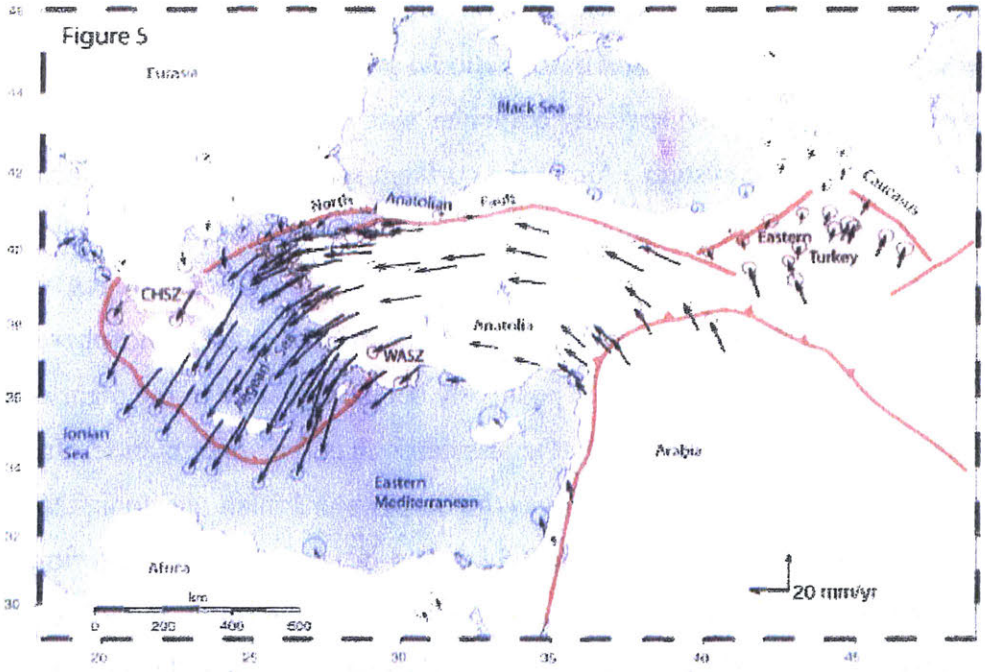

Figure 5 GPS velocities relative to Eurasia. Solid red lines are the boundaries of rigid blocks; shaded pink areas represent broad shear zones. From Royden *et al.* (2003).

Off the western coast of Greece, right-slip on the Kephalonia Transform accommodates the abrupt north-to-south increase in subduction rate along the Hellenic arc. Onshore, the transform is roughly continuous with the Central Hellenic Shear Zone (CHSZ), a broad region of deformation that trends northeastward across southern mainland Greece and the northern Peloponnesus. Displacement across the CHSZ includes components of both dextral shear

(~22 mm/yr) and north-south extension (~9 mm/yr) (reviewed in Royden *et. al.*, 2003). Much of this extension occurs along east- and west-striking normal faults that form active graben systems such as those opening deep-water basins within the Gulf of Corinth and the North Gulf of Evia (Goldsworthy *et. al.*, 2002). To the east, the CHSZ connects with the northeast-striking North Aegean Trough, a much narrower zone of combined extension and shear, and the right-lateral North Anatolian Fault (Royden et. al., 2003; Goldsworthy *et. al.*, 2002). GPS data indicate that the CHSZ and its extensions east (North Aegean Trough) and west (Kephalonia Transform) form the northern boundary of a relatively rigid lithospheric block that is rotating clockwise with respect to Eurasia (and northern Greece). Deformation within this "Aegean block" is largely confined to its boundaries: the southern Hellenic trench to the west and south; the CHSZ to the north; and the West Anatolian Shear Zone to the east (Fig. 5; e.g. McClusky *et. al.*, 2000).

The change in convergence rate and deformational style that occurs across the Kephalonia Transform and the CHSZ spatially coincides with a change in the density of lithosphere entering the Hellenic system. Along the northern segment of the Hellenic arc, downgoing lithosphere underlies the shallow Adriatic Sea. Water depths in this region are between 0 and 1 km; they are less than the typical 2.5 km depth of mid-ocean ridges, where young, oceanic crust is neutrally buoyant with respect to the mantle. Thus, lithosphere subducting beneath the northern Hellenides is positively buoyant relative to the mantle below, probably consisting of continental material that is less dense than the upper mantle. In contrast, subduction along the southern Hellenides involves the deep-water Ionian sea floor. Along this part of the arc, water depths are greater than the 2.5 km mid-ocean ridge depth, varying, on average, from 3 to 4 km and reaching up to 5 km at the trench. In the south, therefore, subducting lithosphere is negatively buoyant relative to the underlying mantle and is likely composed of dense, oceanic materials (Royden *et. al.*, 2003).

North-to-south change in the density of subducting lithosphere along the Hellenic arc is consistent with regional geophysical observations. Gravity data show local positive anomalies over the Aegean Sea, west of the southern Hellenides, suggesting there is mass excess at depth (corresponding to the presence of a dense, subducted slab). Regional gravity anomalies, however, are not observed over the northern Hellenides: there, high-density lithosphere has not descended to depth; the lower plate is likely much more buoyant than in the south (reviewed in

Royden *et al.*, 2003). Complementing these gravity results, seismic tomography shows a high-velocity zone (i.e. a zone of cold, dense material) below the southern Hellenides. The zone dips 45° northeast and penetrates the mantle to the 660 km transition zone (Fig. 6; reviewed in Royden *et al.*, 2003)

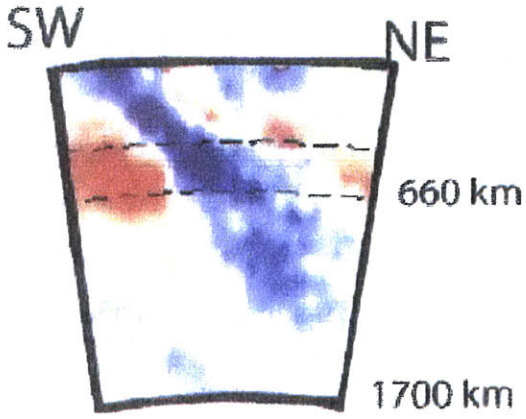

Figure 6 P-wave velocities across the southern Hellenic arc showing a high-velocity zone that dips 45° northeast. Reproduced in Royden *et al.* (2003).

Geologic mapping in mainland Greece and the Peloponnesus indicates the Hellenides have also experienced temporal variability in both density of downgoing lithosphere and subduction rate. Local geology (e.g. the continuity of the older, internal Hellenic thrust sheets over the length of the belt, see Fig. 4) suggests that consumption of continental material at a rate of ~5-10 mm/yr characterized the entire arc from 25-8 Ma. Beginning 4-8 Ma, and approximately synchronous with entry of deep-water oceanic crust into the southern Hellenides, subduction accelerated in the south to its present rate of 40 mm/yr. The east-west trending faults of the Kephalonia Transform and the Central Hellenic Shear Zone that offset the earlier northwest-southeast trending thrusts of the external Hellenides became active during the late Miocene/early Pliocene, probably in response to the changing kinematics of the southern branch of the Hellenic system (reviewed in Royden *et al.*, 2003).

Spatial and temporal coincidence of the transitions from slow to fast subduction rates and buoyant to dense lower-plate materials compellingly suggests a dynamic relationship exists between subduction rate and density of downgoing lithosphere.

PREVIOUS MODELS

Patterns in observational data from the Hellenic arc and other retreating subduction systems guide the development theoretical subduction models designed to construct a comprehensive and quantitative portrait of subduction dynamics. Geodynamic models are a controlled means of examining how various parameters (e.g. subduction rate, slab density, slab rheology) are interrelated. Such models will enable investigation of the relationships among slab density, slab geometry, and mantle flow. At present, few numerical or analog models explicitly address the effect of density on subduction processes. Nevertheless, existing models of retreating subduction systems (e.g. those that explore the interaction of descending slabs with compositional discontinuities in the mantle) provide insight into the advantages and limitations of various modeling techniques.

The usefulness of subduction models depends significantly on their ability to replicate, or at least adjust for, the inherent three-dimensionality of roll-back subduction and trench retreat. As a subducting slab moves through the mantle, the slab displaces ocean-side mantle material, inducing flow into the continent-side mantle wedge (Fig. 7). This transport can occur beneath the slab, but as down-going lithosphere encounters the mantle phase transition at 660 km, below-slab flow paths close off and toroidal flow around the edges of the slab becomes increasingly important (Royden *et al.*, 2003; Kincaid and Griffiths, 2003). Three-dimensional analog modeling has met with some success, but three-dimensional numerical modeling is difficult and time consuming (Royden *et al.*, 2003). In consequence, numerical subduction models have typically considered only two-dimensions, essentially representing cross-sections through retreating slabs. Edge flow cannot be explicitly incorporated into the dynamics of these simulations (Kincaid and Griffiths, 2003).

Enns *et al.* (2003) found that the type of boundary conditions (e.g. periodic versus reflective boundary conditions) applied on the sides of a two-dimensional numerical domain had significant effect on subduction rate and slab geometry. Thus, while applications of specific two-dimensional boundary conditions may be necessary to help compensate for lack of a third dimension, these same conditions may also introduce systematic boundary errors into model outcomes.

Most numerical and analog models of retreating subduction zones are also limited in that they prescribe, rather than calculate, subduction rates and slab geometries. Enns *et al.* (2003), have demonstrated the value (and feasibility) of incorporating these two parameters into numerical models as dependent variables. In their simulations, slab morphologies and trench retreat arise as natural consequences of subduction dynamics, emphasizing the relationships among the shape of subducting lithosphere, retreat rate, and mantle flow. The concept of "self-consistency" is essential to developing simulations that explore the impact of slab density on trench retreat and slab geometry.

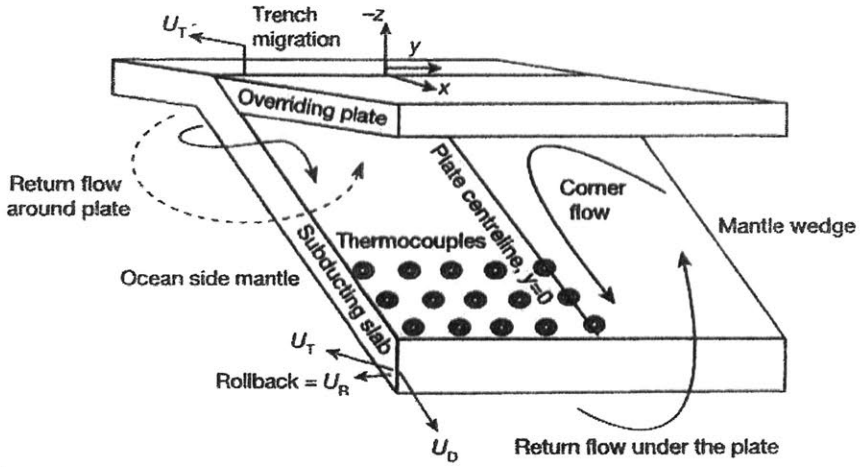

Figure 7 Diagram showing three-dimensional mantle flow around a sinking slab. U_D = down-dip slab velocity; U_T = horizontal trench velocity; roll back velocity $U_R = U_D + U_T$. From Kincaid and Griffith (2003).

In a first attempt to incorporate density variations into simulations of roll-back subduction, Royden (2003) developed a simple, two-dimensional, semi-analytical model of a retreating slab in which lithospheric density is a function of position. Subduction rate and slab shape are unconstrained, allowed to evolve in a manner consistent with subsurface slab-mantle interactions. The model treats the slab as a thin sheet with zero flexural rigidity. Forces acting on the slab are balanced in order to solve for slab velocity given instantaneous slab geometry. These forces are taken to be (1) vertical buoyancy forces proportional to the slab-mantle density contrast; and (2) viscous forces due to mantle flow. Using a Stokes relation for viscous stresses on a rigid body moving through fluid of viscosity μ, shear and normal stresses on the slab are given by $(\mu/\lambda)v_p$ and $(2\mu/\lambda)v_n$ respectively, where v_p and v_n are the slab-parallel and slab-normal components of plate velocity and λ is a characteristic length scale for flow in the mantle.

Royden found that steady-state subduction rates increase with slab density (Fig. 8). Steady-state slab geometry is linear, with shallower dips occurring at higher subduction rates (corresponding to greater slab densities). This unrealistic decrease in slab dip at faster plate velocities suggests dip-angle is strongly controlled by normal stresses acting on the uppermost part of the slab. Entry of buoyant, continental material into the trench behind dense, oceanic material causes subduction rate to drop from 70 mm/yr to <10 mm/yr in 5-10 m.y; the slab steepens to ~90°. If the continental block is longer than ~200 km, low-density material is subducted to ~300 km depth before subduction stagnates (Fig. 9 left). Oceanic material subducted behind continental blocks shorter than 200 km causes the slab to shallow out again and subduction rates to return to 70 mm/yr within 20-30 m.y (Fig. 9 right).

Royden's model is self-consistent, but the fluid dynamics are oversimplified. The challenge for new density-variable subduction models is to find a more realistic representation of the viscous forces acing on a subducting slab.

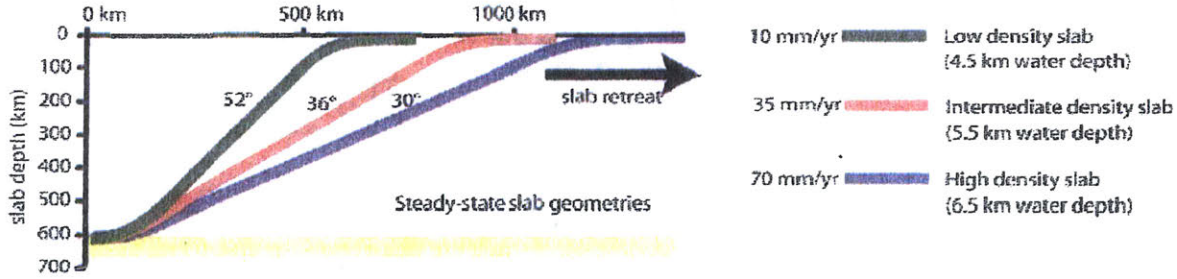

Figure 8 Steady-state slab geometries and subduction rates for low-, intermediate-, and high-density slabs. From Royden *et al.* (2003).

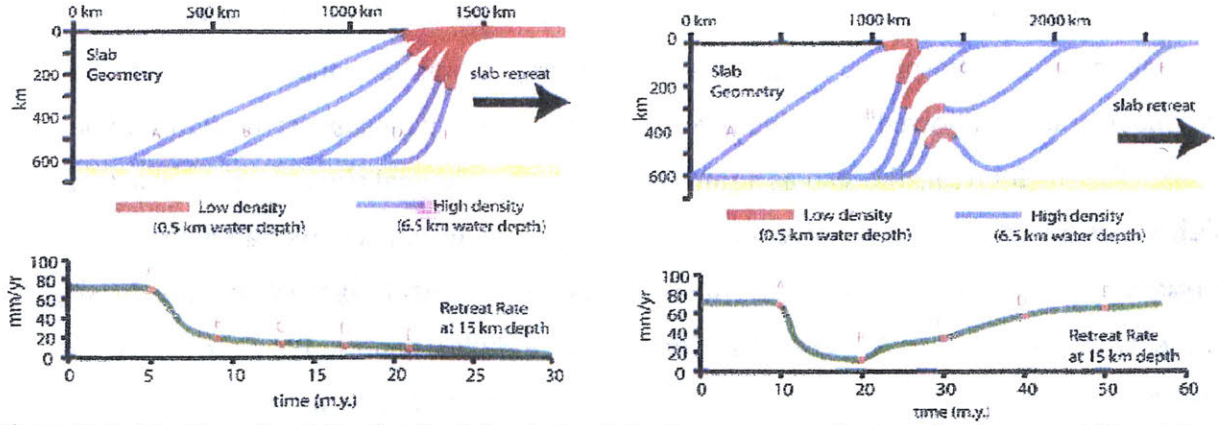

Figure 9 Subduction of variable-density slabs. Left: subduction stagnates after low-density material is subducted to ~300 km depth. Right: Subduction rate slows and slab steepens after entry of a 200 km-long, low-density block. Subsequent entry of high-density material causes subduction rate to increase to its original value. Bottom row shows rate of slab roll-back computed by tracking the slab position at 15 km depth. From Royden *et al.* (2003).

METHODS

Subduction of cold, dense oceanic lithosphere is an expression of thermal convection in the mantle. This study explores the movements of a subducting slab in steady-state retreat via numerical simulation of mantle convection. The mantle is treated as an incompressible, very viscous fluid. In the infinite Prandtl number limit (kinematic viscosity >> thermal diffusivity), the equations governing mantle convection are

Stokes equation: $$\nabla^2 \vec{u} = \nabla p + \mathrm{Ra} T \hat{k} \quad \text{(conservation of momentum);} \tag{1}$$

heat transfer: $$\frac{\partial T}{\partial t} + \vec{u} \cdot \nabla T = \nabla^2 T \quad \text{(conservation of energy);} \tag{2}$$

and incompressibility: $$\nabla \cdot \vec{u} = 0 \quad \text{(conservation of mass),} \tag{3}$$

where $\hat{k}$ is the unit vector in the vertical direction (defined positive upward), $\vec{u}$ is dimensionless velocity, p is dimensionless pressure, T is dimensionless temperature, and t is dimensionless time. All dimensional parameters are combined in the Rayleigh number,

$$\mathrm{Ra} = \frac{\rho_0 g \alpha \Delta T D^3}{\kappa \mu}.$$

For convection in the mantle, ρ_0 is density at the upper surface of the mantle layer, g is gravitational acceleration, α is the coefficient of thermal expansion, $\Delta T = T_{base} - T_{surface}$ is the temperature difference across mantle layer, D is the depth of the mantle layer, κ is thermal diffusivity, and μ is dynamic viscosity. The equations of momentum, energy, and mass are solved using ConMan, a finite element code for two-dimensional, incompressible convection in a Cartesian domain.[2]

[2] Not all parameters contained in the Rayleigh number are explicitly input into ConMan. The code calculates the non-dimensional depth of the mantle layer (D') from grid geometry and the dimensionless temperature drop across the layer ($\Delta T'$) from temperature boundary conditions. A normalized reference viscosity μ_0' and normalized thermal diffusivity κ' are specified directly. Density enters as part of a normalized "thermal buoyancy number" defined as $(\rho_0 g \alpha)'$. In this study, $D' = \Delta T' = \mu_0' = \kappa' = 1$; thus, $(\rho_0 g \alpha)' = \mathrm{Ra}$. Changes in density, therefore, must be input in terms of corresponding changes in Rayleigh number.

Variables in Equations 1-3 are non-dimesionalized using length scale D, time scale D^2/κ, and mass scale $\mu D^3/\kappa$. This leads to the following set of dimensionless variables (primed):

$$x' = \frac{x}{D} \text{ and } t' = t\frac{\kappa}{D^2}, \text{ from which it follows } \vec{u}' = \vec{u}\frac{D}{\kappa};$$

$$T' = \frac{T - T_{surface}}{\Delta T}; \text{ and}$$

$$p' = (p - P_0)\frac{D^2}{\mu_0 \kappa},$$

where P_0 is lithostatic pressure and μ_0 is mantle viscosity at $T = T_{base}$. In this study, all reference parameters except surface density are held constant; the values chosen for these parameters are shown in Table 1.

Symbol	Quantity	Value
ρ_0	Density at $T = T_{surface}$	3300 kg/m^3 (runs 1-3 & 6)
		2800 kg/m^3 (runs 4 & 5)
g	Gravitational acceleration	10 m/s^2
α	Coefficient of thermal expansion	3×10^{-5} K^{-1}
ΔT	Temperature drop across convecting system	2000 K
D	Depth of convecting system	6.6×10^5 m
κ	Thermal diffusivity	10^{-6} m^2/s
μ_0	Dynamic viscosity at $T = T_{base}$	10^{21} Pa s
Ra	Rayleigh number ($\rho_0 g\alpha \Delta T D^3/\kappa\mu_0$)	5.7×10^5 (runs 1-3 & 6)
		4.8×10^5 (runs 4 & 5)

Table 1 Values of reference parameters used in calculations. The values are reasonable for the upper mantle (Turcotte and Schubert, 2002). The lower limit of the model domain is set at the 660-km seismic discontinuity because phase change in the mantle at this depth impedes flow across the boundary.

Viscosity is allowed to vary inversely with temperature according to

$$\mu(T) = \mu_0 \exp\left[\frac{E_a}{R\Delta T}\left(\frac{1}{T + T_0} + \frac{1}{1 + T_0}\right)\right] \text{ for } \mu < \mu_{\max}, \quad (4)$$

where E_a is activation energy, $R = 8.31$ J mol^{-1} K^{-1} is the universal gas constant, and $T_0 = 273/\Delta T$. The viscosity of low-temperature material is capped at μ_{max}. Requirement of temperature-dependent viscosity makes the cold, downgoing slab stronger than the surrounding mantle, ensuring the slab moves as a coherent plate. For all runs, activation energy is set to 100 kJ mol^{-1}. This value is large enough to produce significant viscosity contrast (several orders of magnitude) between hot material at the base of the mantle layer and cold lithosphere at the top, but it is not so large that the entire system becomes stiff and immobile (Conrad and Hager, 2001).

The model domain is a rectangular grid with aspect ratio 5 (660 km deep and 3300 km wide) and resolution 29 × 145 elements. Horizontal velocity boundary conditions are periodic on the sides of the box and free-slip on the top of the box. A constant horizontal velocity v_p is imposed along the bottom surface (see below). Temperature is fixed along the base of the grid ($T = T_{base}$) and top of the grid ($T = T_{surface}$, where $T_{surface} < T_{base}$), corresponding to non-dimensional temperature $T' = 1$ at the base and $T' = 0$ at the top. Below the upper surface, a thermal boundary layer, ~70 km (3 elements) thick represents the lithosphere. Temperature within this layer is initially uniform ($T' = 0$) but is allowed to evolve with time. Initial temperature of the underlying mantle is everywhere set to $T' = 1$ in order to prevent formation of instabilities at the bottom of the box. The base of the lithosphere is maintained at $T' = 1$.

The grid is divided into three rheologically distinct regions (Fig. 10): (1) the mantle and most of the lithosphere (temperature-dependent viscosity); (2) a small weak zone in the overriding plate; and (3) a "subduction zone" (also weak) designed to drive the lower plate into the mantle at the plate margin. The viscosity of material in regions 1 and 2 increases exponentially with decreasing temperature according to Equation 4. In region 1, maximum viscosity is set at $\mu_{max} = 1000\mu_0$, such that the cold lithosphere forms a strong layer above the mantle. In region 2, viscosity is capped much lower: $\mu_{max} = 10\mu_0$. This low-viscosity zone (10 elements wide and 3 elements deep) is placed within the upper plate, adjacent to the subduction zone. The region allows the upper plate to pull away from the downgoing plate and thus incorporates into the model a mechanism for "back-arc" extension.

The subduction zone (5 elements wide and 3 elements deep) is a region of uniform, very low viscosity ($\mu = .01\mu_0$) that facilitates localized deformation of the lower plate as it bends and descends into the mantle. Horizontal velocity conditions imposed on the right side of the

subduction zone drive cold material into the region at speed v_p.[3] Material is driven out of the bottom of the subduction zone at the same speed v_p such that the net volume flux through the region is zero (Fig. 11). This weak-zone "subduction machine" has no natural counterpart.

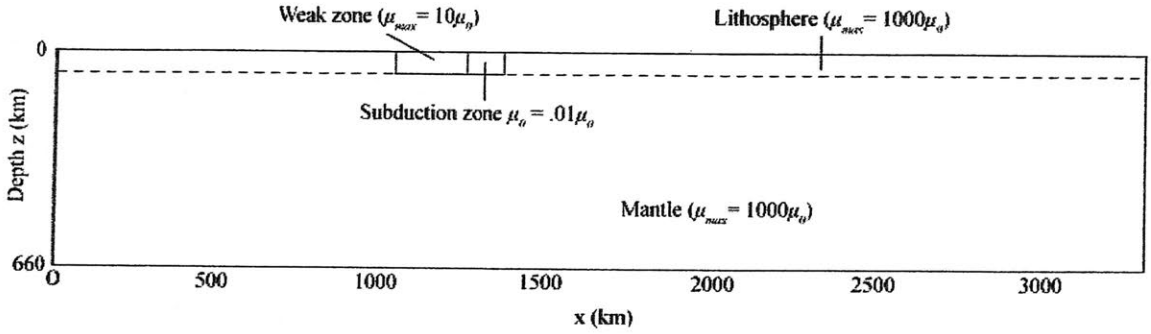

Figure 10 Diagram showing material properties of different regions in the model domain. The mantle, lithosphere, and "weak zone" all have temperature-dependent viscosity according to Equation 4. Viscosity contrast between the lithosphere and mantle is capped at three orders of magnitude; viscosity contrast between the weak zone and mantle is limited to a factor of 10. Viscosity in the subduction zone is held constant at $.01\mu_0$.

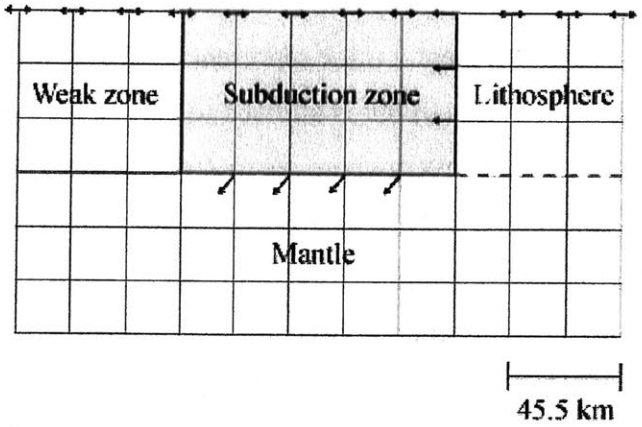

Figure 11 Diagram showing velocity boundary conditions in the "subduction zone." Imposed velocities are designed to drive lithospheric material into the subduction zone and guide it out of the bottom of the region into the mantle. Single-headed arrows show the direction of imposed velocities; double-headed arrows represent free-slip conditions on the upper surface of the grid. All imposed velocities have magnitude v_p. Material is forced out of the subduction zone along a length chosen such that the slab has the same thickness entering and exiting the region. Figure modified from Figure 2 of Conrad and Hager (2001).

Rather, it is a convenient way to numerically produce stable subduction (e.g. Conrad and Hager, 2001; Chen and King, 1997). Thus, the angle at which material is forced out of the subduction zone is not inherent to the model. In this study, two angles are chosen (45° and 90°) to explore

[3] The base of the mantle layer is also forced to move with horizontal velocity v_p so that the subduction zone remains in the center of the model domain.

how the direction in which material exists the subduction zone affects the evolution of the subducting slab.

The plate velocity v_p is prescribed and remains fixed throughout each model run. The model, therefore, is not inherently self-consistent: retreat velocities are imposed rather than computed from mantle flow. Steady-state, dynamically consistent retreat rates (and slab geometries) are determined iteratively instead. The range of possible values of v_p is narrowed based on results of successive runs. The criteria for converging on retreat velocity is loose: if v_p is too large, the resulting flow field "pushes" the slab laterally, artificially imposing stresses on the downgoing lithosphere; if v_p is too small, the negative buoyancy of the slab causes it to sink vertically downward. To examine the effect of density on trench velocity, steady-state retreat rate was approximated for two systems with different slab-mantle density contrasts.[4] For Runs 1-3 and 6, the density difference between surface lithosphere and the underlying mantle is $(\rho_0 - \rho_1) = 198$ kg/m^3, where ρ_1 is density at $T' = 1$. For Runs 4 and 5, $(\rho_0 - \rho_1) = 168$ kg/m^3. Table 2 summarizes the input parameters for these six runs.

Run	Angle at which slab is forced out of subduction zone	Rayleigh number ($\times 10^5$)	Dimensionless plate velocity v_p
1	90	5.7	450
2	90	5.7	200
3	90	5.7	340
4	90	4.8	300
5	90	4.8	340
6	45	5.7	340

Table 2 Model parameters for cited runs. Ra = 5.7×10^5 corresponds to $\rho_0 = 3300$ kg/m^3; Ra = 4.8×10^5 corresponds to $\rho_0 = 2800$ kg/m^3. The values of ΔT, D, κ, and μ_0 are the same for all runs and are given in Table 1.

[4] Density change $\Delta\rho$ due to temperature change ΔT is given by $\Delta\rho = -\rho_0 \alpha \Delta T$. The buoyancy force per unit volume ($\vec{F}_B$) depends only on local density contrast: $\vec{F}_B = \Delta\rho \vec{g}$. Two values are chosen for ρ_0: 3300 kg/m^3 (Runs 1-3 and 6) and 2800 kg/m^3 (Runs 4 and 5).

RESULTS

The finite element model used in this study sets up a simple "machine" for numerical simulation of stable subduction. The model is designed to explore how changes in slab buoyancy affect the steady-state geometry and retreat velocity of subducting lithosphere. Described below are results for two retreating subduction systems with different slab-mantle density contrasts: (1) $(\rho_0 - \rho_1) = 198$ kg/m^3 and (2) $(\rho_0 - \rho_1) = 168$ kg/m^3, where $(\rho_0 - \rho_1)$ is the difference between density at $T' = 0$ (lithosphere) and density at $T' = 1$ (mantle).

The artificial mechanism of driving lithosphere into the mantle via imposed velocities along the boundaries of a weak "subduction zone" raises another question: Does the angle at which cold material exits the subduction zone impact the steady-state behavior of the slab? Comparison of results for two angles (45° and 90°) shows the direction of imposed velocity does not have a significant impact on either retreat rate or slab geometry.

Slab-Mantle Density Contrast $(\rho_0 - \rho_1) = 198$ kg/m^3

Figures 12, 13, and 14 show the temporal evolution of a dense slab driven at velocity $v_p = 21.5$ mm/yr, $v_p = 9.5$ mm/yr, and $v_p = 16.2$ mm/yr respectively. Each figure presents time-sequential "snap shots" of the mantle temperature field. Together, the figures illustrate the qualitative criteria used to converge on a dynamically consistent, steady-state retreat velocity (v_r). In all three runs (Runs 1, 2, and 3), the slab heats up and loses definition at depth. Nevertheless, it is possible to extract general patterns of behavior for three cases: (1) $v_p > v_r$ (Run 1); (2) $v_p < v_r$ (Run 2); and (3) $v_p \approx v_r$ (Run 3). All model parameters are invariant between runs except imposed plate velocity. To simulate subduction of a dense, oceanic plate, density at $T' = 0$ is set to 3300 kg/m^3 (Ra = 5.7×10^5), corresponding to a slab-mantle density contrast of 198 kg/m^3. Material is driven out of the subduction zone at 90°.

Case (1): $v_p > v_r$

The arcuate shape of the slab shown in Figure 12 ($v_p = 21.5$ mm/yr) is typical of slabs driven faster than the intrinsic steady-state retreat rate of the system. The strong lateral component of slab velocity induces horizontal flow beneath the descending lithosphere (Fig. 15A). At depth, where the slab interacts with this flow, dip angle decreases such that

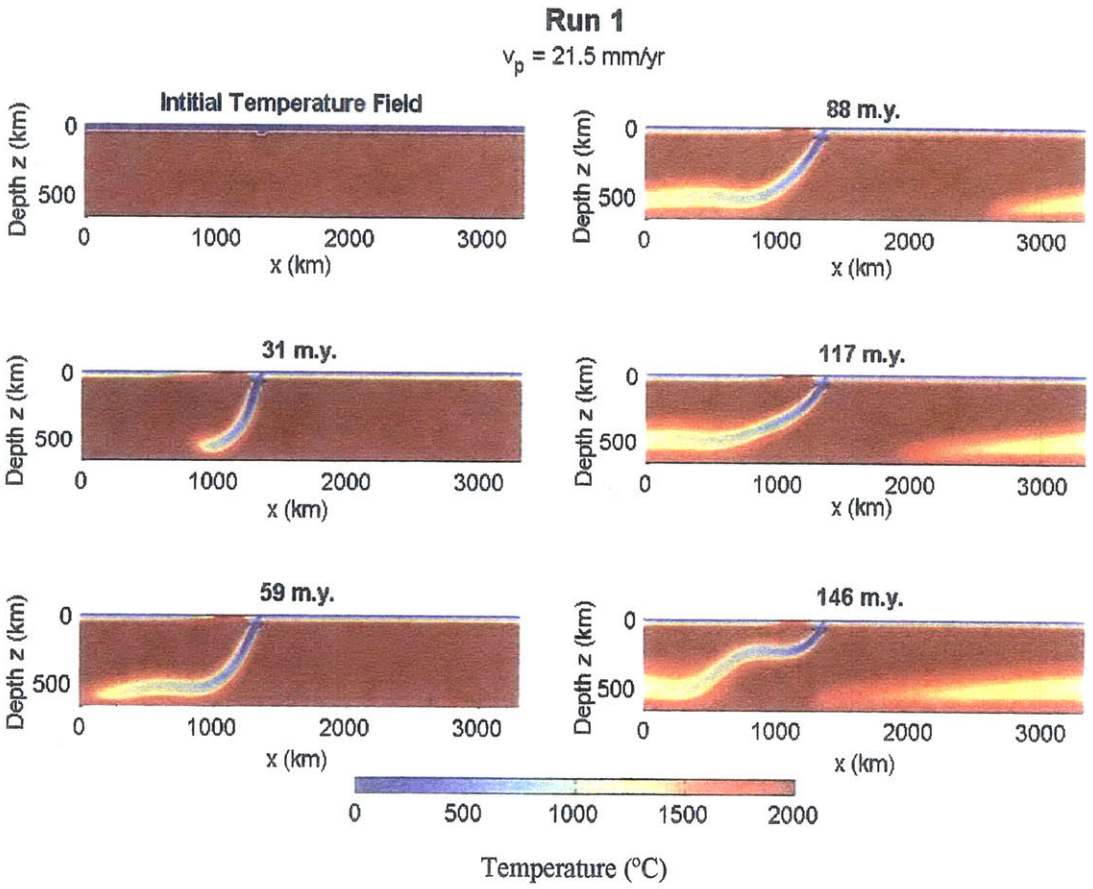

Figure 12 Evolution of a negatively buoyant slab ($\rho_0 - \rho_1$ = 198 kg/m^3) driven at v_p = 21.5 mm/yr (Run 1). Material is forced out of the subduction zone at 90°. The slab has a general arcuate shape due to strong horizontal flow beneath the descending lithosphere. Slab geometry is characteristic of lithosphere driven faster than the intrinsic steady-state retreat rate of the system.

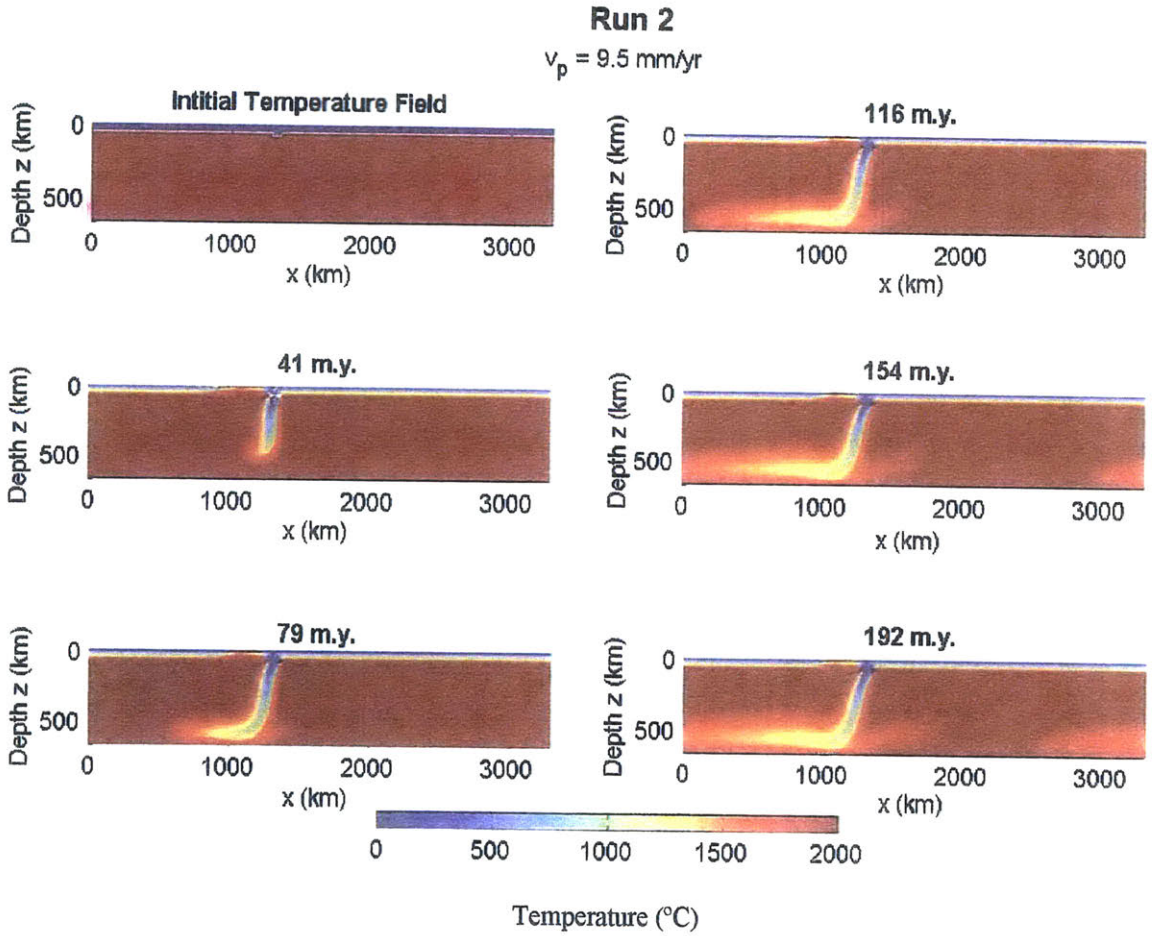

Figure 13 Evolution of a negatively buoyant slab ($\rho_0 - \rho_1$ = 198 kg/m^3) driven at v_p = 9.5 mm/yr (Run 2). Material is forced out of the subduction zone at 90°. The slab is sigmoidal, steepening from ~60° near the surface to ~75° at depth. Below several hundred kilometers, vertical buoyancy forces overwhelm lateral viscous forces set up by imposed velocities in the "subduction zone." Slab geometry is characteristic of lithosphere driven slower than the intrinsic steady-state retreat rate of the system.

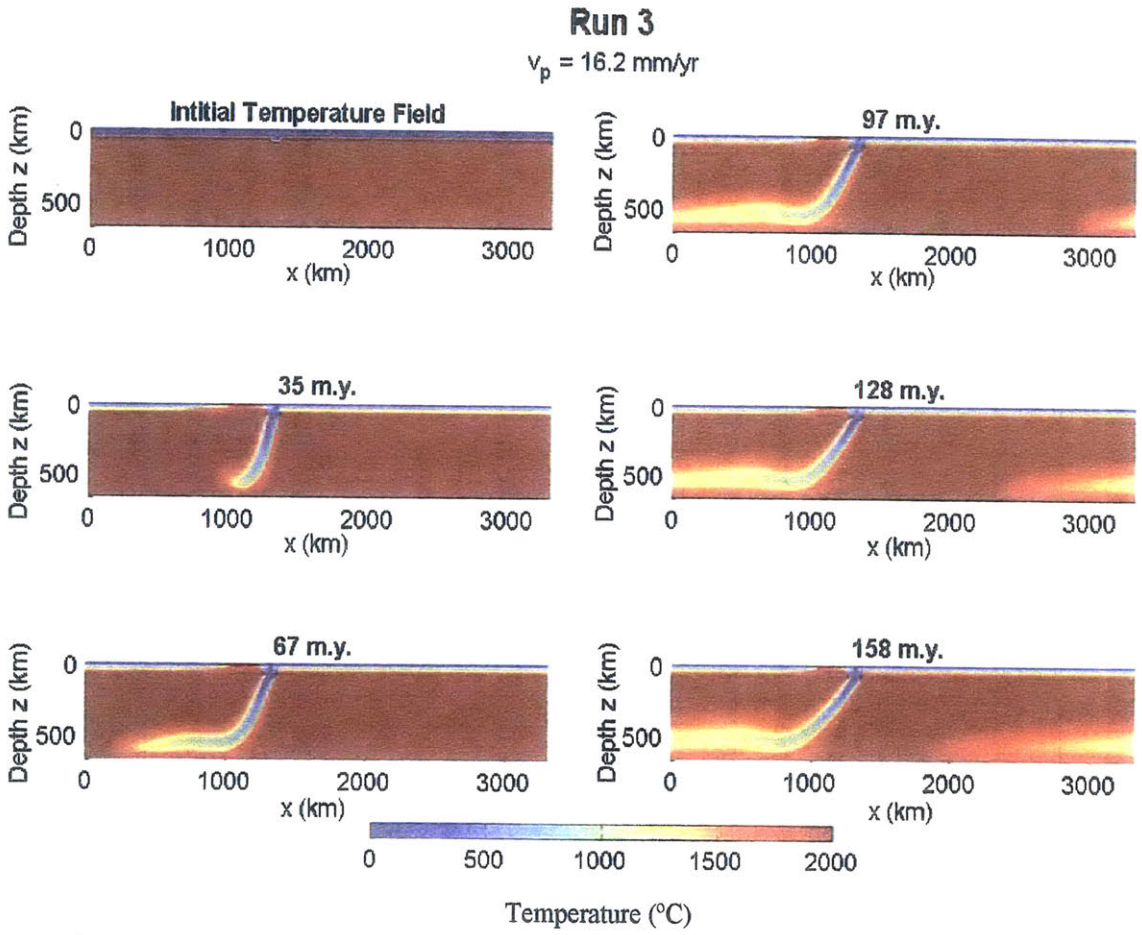

Figure 14 Evolution of a negatively buoyant slab ($\rho_0 - \rho_1$ = 198 kg/m^3) driven at v_p = 16.2 mm/yr (Run 3). Material is forced out of the subduction zone at 90°. Imposed plate velocity is inferred to be approximately equal to the intrinsic steady-state retreat rate of the system. Steady-state slab geometry is roughly planar, dipping ~50°.

overall slab geometry is concave upward. Increase in plate velocity causes increase in slab curvature; slabs driven at sufficiently large velocities do not penetrate the mantle more than a few hundred kilometers but instead arc back upward toward the surface.

In the mantle ("hot spot") reference frame, rather than the moving reference frame in which the model operates[5], flow beneath the slab represents "return flow" generated by rapid, oceanward retreat of the downgoing plate. As the slab "rolls back," material is forced out of the high-pressure area behind the slab into the low-pressure region below the upper plate.

Upwelling of hot mantle material into the back-arc "weak zone" occurs as the rigid part of the overriding plate pulls away from the trench. This upward flow of "asthenosphere" into the upper 100 km of the model domain represents localized extension and thinning of the upper plate (basin formation). This behavior is not unique to systems with high imposed plate velocities. It occurs in all runs.

It is clear from the three velocity plots in Figure 15, however, that the lithosphere is also extending along its entire length: surface velocities approach zero with distance from the subduction zone. At the surface, therefore, the lithosphere does not act like a rigid plate as desired but rather deforms internally. Occurrence of widespread surface deformation suggests the viscosity of the lithosphere may have been capped too low; μ_{max} may be better set to $10^4\mu_0$.

Case (2): $v_p < v_r$

The slab shown in Figure 13 (v_p = 9.5 mm/yr) has sigmoidal geometry, suggesting the prescribed plate velocity is smaller than the intrinsic retreat rate of the slab. Near the surface, where velocity boundary conditions drive flow, the slab dips ~60°[6]; by 200 km depth, dip-angle increases to ~75°. In this case, slab-steepening is likely an expression of downward-decreasing sensitivity to imposed surface velocities (because these velocities are very small). At depth, downward-directed buoyancy forces dominate over lateral viscous forces set up by the subduction zone, and the slab bends toward vertical. Between ~200 and 500 km depth, velocities in the center of the slab have a strong

[5] Again, the model adopts a reference frame that moves relative to the mantle at the same velocity as the trench (v_p). In this "retreating" frame, the position of the subduction zone stays fixed at the center of the model domain.

[6] Slab dip is calculated based on the slope of the line through the coldest part of the slab.

vertical component (Fig. 15B). Below ~500 km, interaction with the base of the mantle layer (representing the 660-km seismic discontinuity) causes the slab to flatten out.

A)

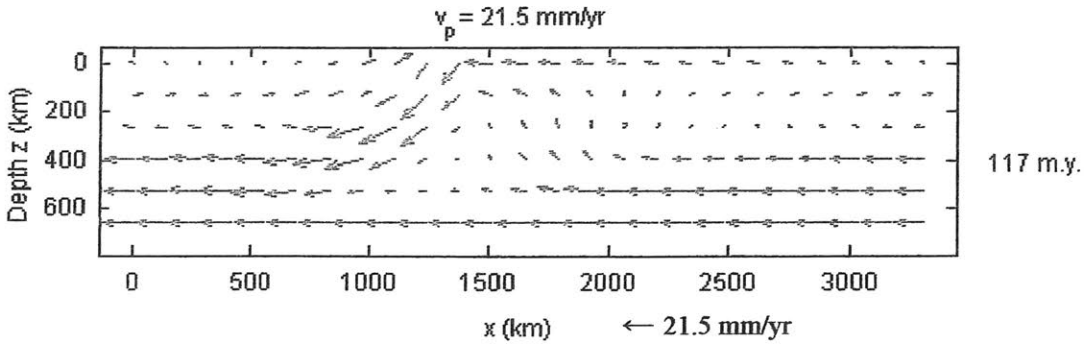

B)

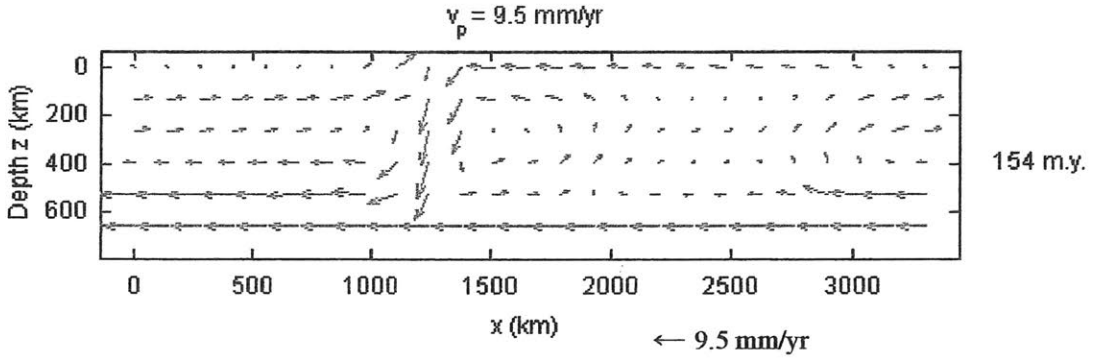

C)

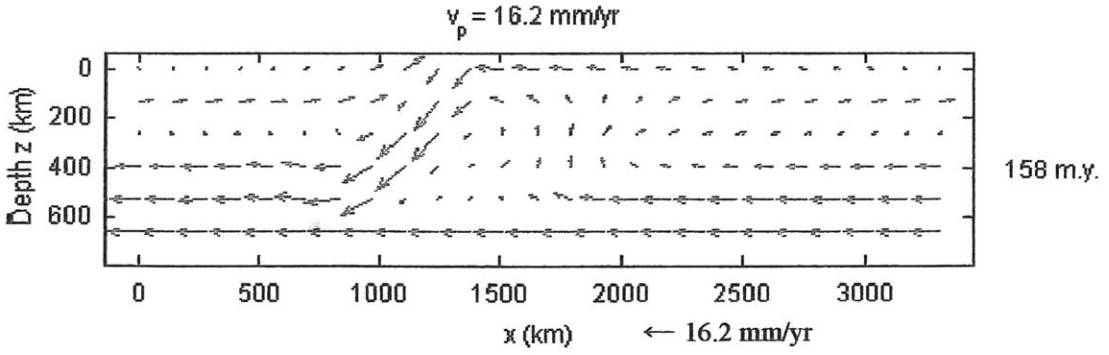

Figure 15 Velocity fields for flow in the upper mantle. A) $v_p > v_r$ (Run 1): Strong horizontal flow beneath the descending lithosphere lifts the slab from the base of the mantle layer. B) $v_p < v_r$ (Run 2): Velocities in the center of the slab are nearly vertical due to the dominance of downward-directed buoyancy forces over lateral viscous forces. C) $v_p \approx v_r$ (Run 3): Slab descends linearly to the base of the mantle layer in the absence of rapid "return flow." Mantle material below the downgoing plate flows "seaward," away from the trench.

Case (3): $v_p \approx v_r$

Slabs driven faster and slower than the intrinsic steady-state retreat rate of the system behave in consistently and characteristically different ways (upward-arcing slab geometry and strong lateral flow beneath the slab versus downward-steepening dip-angle and near vertical flow in the center of the slab). Slab behavior thus acts as a guide in converging on a dynamically consistent plate velocity v_r. For Ra = 5.7×10^5, $v_r \approx 16$ mm/yr (Fig. 14). The slab is essentially planar, with a steady-state dip of ~50°. Roll-back motion does not set up a large return flow as it does beneath more rapidly retreating slabs (Fig. 15C), allowing the lithosphere to descend linearly to the base of the model domain. Instead, mantel material beneath the downgoing plate flows oceanward (away from the trench).

Figure 16 shows steady-state slab-normal (top) and slab-parallel (bottom) viscous stresses for $v_p = 16.2$ mm/yr. At shallow depths, where the negative buoyancy of the descending lithosphere "pulls" the slab downward, down-dip stresses are tensional (positive). Around 300 km depth, down-dip stresses change sign: the slab experiences compression as it encounters, and is unable to penetrate, the 660-km discontinuity (base of the model domain). The small compressional region at the top of the slab is probably associated with bending of the lithosphere as it leaves the subduction zone. Normal stresses are largest in the center of the slab, dropping significantly at the slab edges.

In contrast, shear stresses are roughly antisymmetric about the down-dip axis of the slab, approaching zero near the slab center. The symmetry of shear stresses reflects the coherence of the subducting lithosphere: shear is small in the cold, rigid interior of the slab and much larger along the edges, where the downward moving lithosphere drags adjacent mantle material toward the base of the convecting system.

The numerically-derived, steady-state retreat rate of 16 mm/yr is small compared to subduction rates along retreating boundaries in the Mediterranean region. Where dense, oceanic lithosphere enters the southern Hellenides, for example, subduction occurs at ~40 mm/yr. In part, the low retreat velocity of the numerical subduction system may be due to the values chosen for certain reference parameters (e.g. mantle viscosity, which was set high: $\mu_0 = 10^{21}$ Pa s).

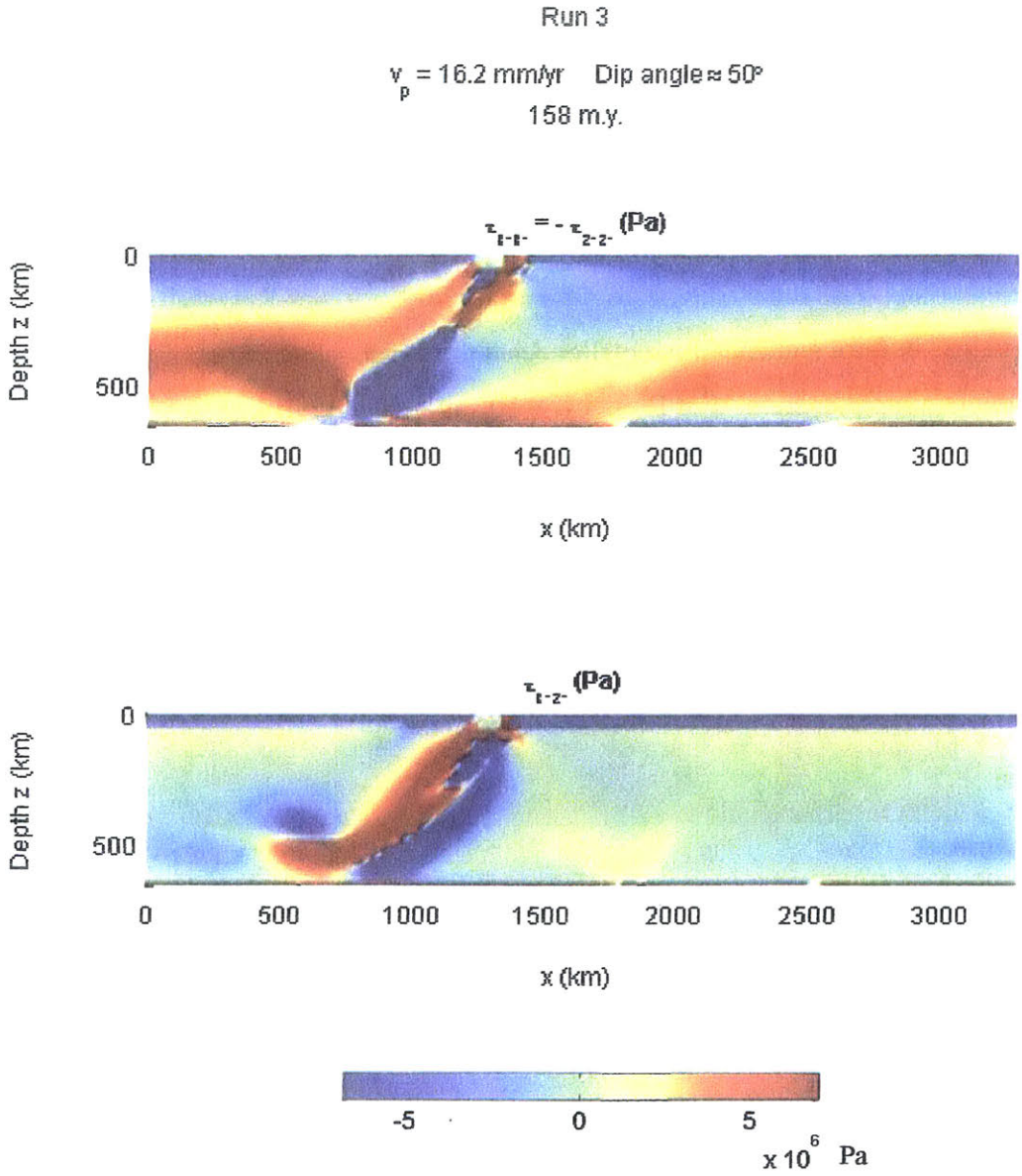

Figure 16 Slab-normal (top) and slab-parallel (bottom) stresses computed for steady-state mantle flow around a dense , retreating slab (Run 3, vp = 16.2 mm/yr). Slab dips ~50°. Positive x'-axis lies in the up-dip direction. Positive normal stresses are tensional; negative normal stresses are compressional.

Slab-Mantle Density Contrast ($\rho_0 - \rho_1$) = 168 kg/m^3

To examine the influence of slab buoyancy on steady-state retreat rate, the iterative process for converging on v_r is repeated with surface density ρ_0 set to 2800 kg/m^3 (Ra = 4.8 × 10^5). The slab-mantle density contrast for this lower-Rayleigh number system is ~15% smaller than the corresponding density contrast in Runs 1-3. It is therefore expected that the steady-state retreat rate for Ra = 4.8 × 10^5 should be ~15%

slower than the steady-state retreat for Ra = 5.7×10^5. As before, material is forced out of the subduction zone at 90°.

Figure 17 compares the results (both calculated around time 150 m.y. for plate velocity v_p = 16.2 mm/yr) of the lower- and higher-Rayleigh number systems. For Ra = 5.7×10^5 (Fig. 17A), $v_p \approx v_r$, and the slab is roughly planar. Slab geometry is nearly identical for Ra = 4.8×10^5 (Fig. 17B). Slight increase in slab curvature with decrease in Rayleigh number suggests the steady-state retreat rate for the lower-Rayleigh number system is smaller, but not significantly smaller, than the steady-state retreat rate for the higher-Rayleigh number system. For Ra = 4.8×10^5, $v_r \approx 14$ mm/yr; trench velocity is ~15% slower than 16 mm/yr as predicted.

A)

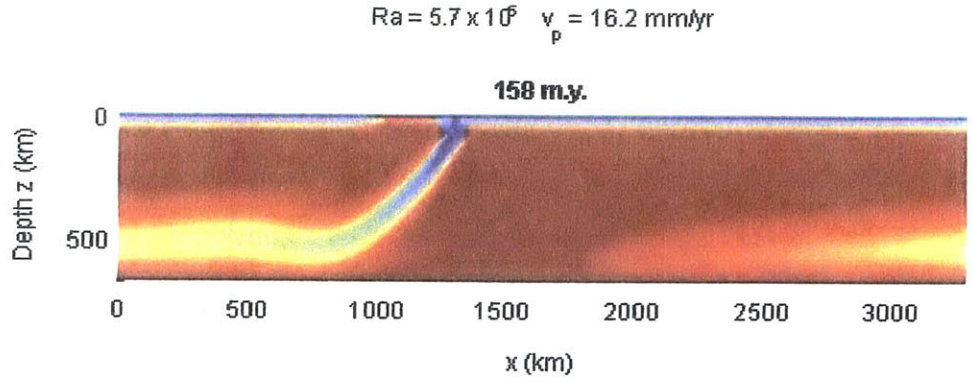

B)

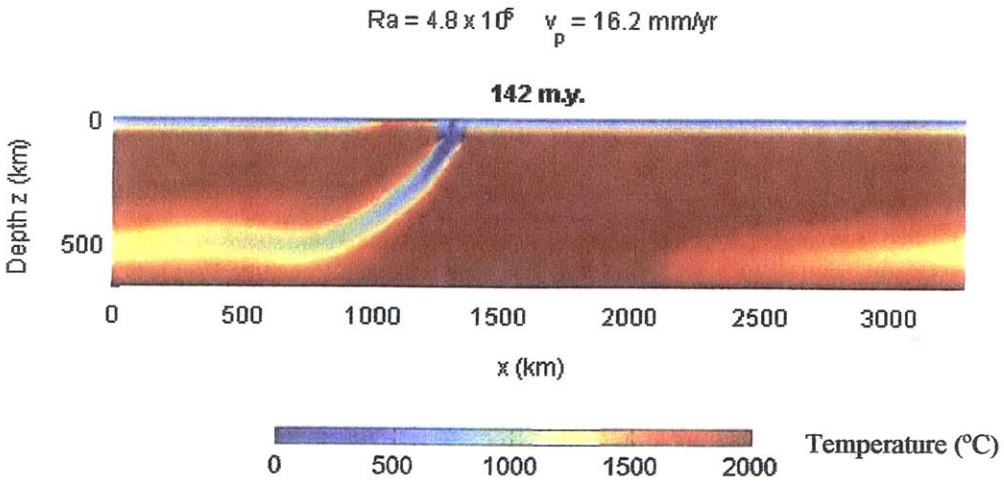

Figure 17 Comparison of slab geometries for (A) Ra = $5.7 \times 10^5$and (B) Ra = 4.8×10^5. Imposed plate velocity is the same for both runs (v_p = 16.2 mm/yr). Temperature fields are computed for time $t \approx 150$ m.y.

Angle of Imposed Velocity

The usefulness of numerical simulations depends on understanding how model design affects results in ways that have no natural analog. Concentrating deformation of downgoing lithosphere within a localized, uniformly weak "subduction zone" and guiding material into and out of this subduction zone using imposed velocity boundary conditions are artificial means of generating realistic subduction. Thus, the geometry of the "subduction zone" and the choice of velocity boundary conditions are somewhat arbitrary. It is therefore important to explore how the orientation of velocity conditions in the subduction zone influences the behavior of subducting lithosphere.

Figure 18 shows the geometry of a slab forced out of the subduction zone at 45° (Run 6). Prescribed plate velocity (v_p = 16.2 mm/yr) and all material properties (e.g. slab buoyancy, reference viscosity, thermal diffusivity) are the same as in Run 3. The two runs differ only in the orientation of velocities imposed on the lower boundary of the subduction zone (45° versus 90°). The slabs in both runs are in steady-state, migrating "seaward" at a dynamically consistent retreat rate. Unlike the slab in Run 3, however, the slab in Run 6 has nonplanar geometry (compare Fig. 18 with Fig. 14). Near the surface, the slab is driven down into the mantle at 45°; at depth, the slab steepens and straightens to ~50°. The lower part of the slab dips at roughly the same angle as the slab in Run 3, suggesting that in the deeper part of the model domain, the influence of imposed shallow-level velocities diminishes and the slab approaches a dynamically consistent geometry. The similarity of Runs 3 and 6 indicates the orientations of velocities imposed in the subduction zone do not significantly impact the steady-state behavior of downgoing lithosphere.

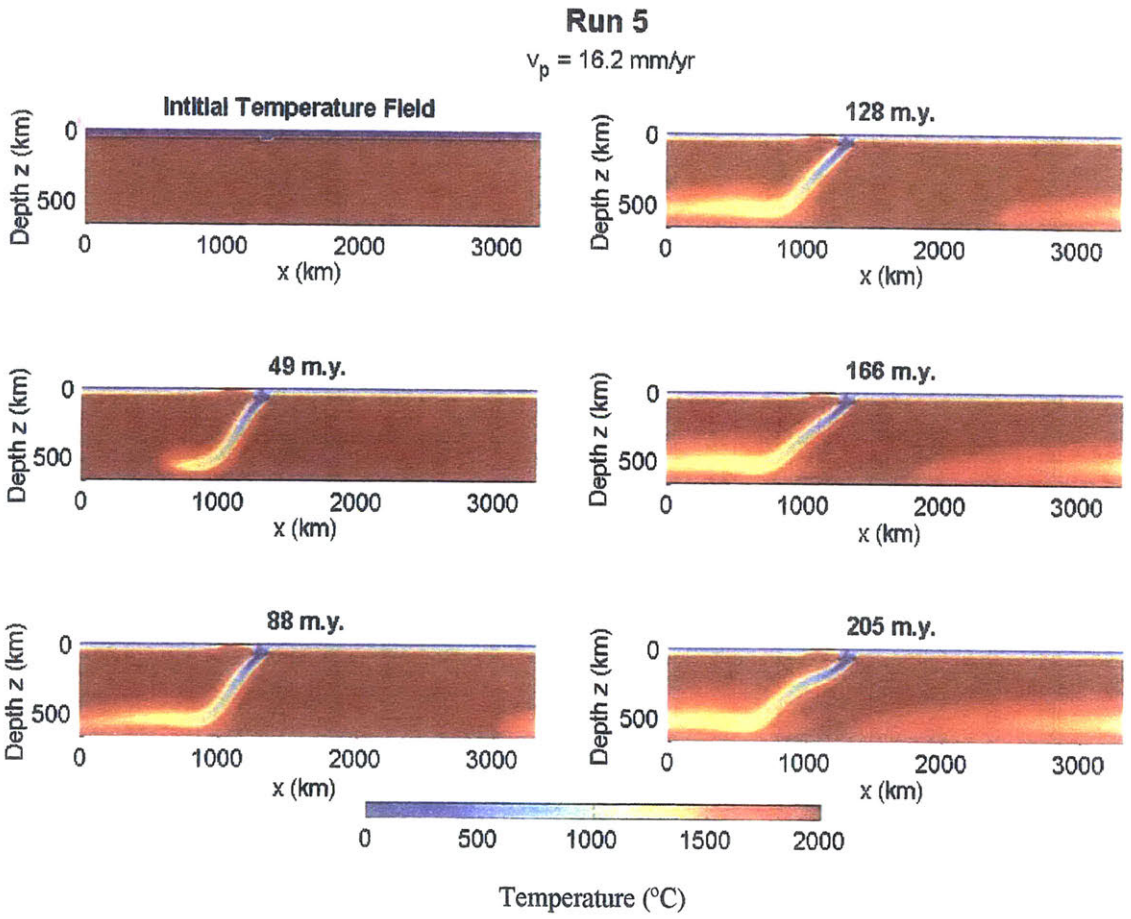

Figure 18 Evolution of a negatively buoyant slab ($\rho_0 - \rho_1$ = 198 kg/m^3) driven at v_p = 16.2 mm/yr (Run 6). Material is forced out of the subduction zone at 45°. Imposed plate velocity is inferred to be approximately equal to the intrinsic steady-state retreat rate of the system. The slab dips ~45° near the surface; at depth, where the influence of imposed surface velocities is less significant, the slab steepens to ~50° . Upwarping of the slab at time 205 m.y. is due to interaction of the slab tip with the descending lithosphere.

DISCUSSION AND CONCLUSIONS

This study uses a finite element code for two-dimensional, incompressible convection (ConMan) to model roll-back subduction of cold, viscous lithosphere in a uniform viscous mantle. The model provides a basic framework in which to explore how the dynamic interactions between downgoing lithosphere and surrounding mantle are expressed in mantle flow patterns and slab geometry. The project is intended as a starting point for theoretical investigation into the role of density in the subduction process. The results of this study suggest finite element, viscous flow modeling is potentially a powerful tool for quantitatively understanding the relationships among density of subducting lithosphere, slab geometry, trench retreat, and mantle flow. With this end goal in mind, several shortcomings of the model here presented are immediately clear.

In order to examine how retreat rate and slab morphology evolve naturally from slab-mantle density contrasts, the most useful numerical models will compute these features rather than prescribe them *a priori*. The present study, however, imposes plate velocity, then determines whether this velocity is slower or faster than the "intrinsic" retreat rate of the system. Criteria for this assessment are loose and qualitative (slab geometry, direction of mantle flow). Quantifying these criteria would improve confidence in iteratively determined steady-state retreat rates. For example, stresses on a slab in steady-state retreat should balance. Thus, calculation of net stress on a model slab would illuminate any stresses "artificially" introduced by imposed surface velocities and thereby guide the next choice of plate velocity. Moreover, with a quantitative means for evaluating the dynamic consistency of imposed velocities, it may be possible to incorporate an iterative procedure into the code such that given an initial plate velocity, the program converges to a consistent, steady-state retreat rate.

An inherently self-consistent model (no prescribed velocities) is perhaps more difficult to develop. The problem is how to generate stable subduction without directly guiding lithosphere into the mantle via velocity boundary conditions. A potential solution is to extend the low-viscosity "subduction zone" a short distance into the mantle. If initial temperature in this region is set to $T' = 0$, gravitational instability will cause lithospheric downwelling even in the absence of imposed velocities. In order to produce asymmetric subduction, the boundary between the

subduction zone and adjacent upper-plate "weak zone" must be pinned. Chen and King (1998) found the geometry of the subduction zone (e.g. a 90°-dipping zone versus a 45°-dipping zone) does not significantly affect the geometry of the subducting slab. This alternative set-up would allow surface velocities (and thus the rate of trench migration) to evolve freely to their steady-state values.

The model developed in this study is also limited in the type of slab-mantle density contrasts that can be reproduced. Currently, the model can only simulate negatively buoyant lithosphere. This restriction is significant for studies of density-driven subduction, which seek to compare the behavior of positively and negatively buoyant lithosphere at subduction boundaries. Moreover, the problem is not easily fixed. The model considers the mantle and lithosphere to be the same material because the values of all material reference parameters (e.g. μ_0, ρ_0, α, κ) are identical in the two regions. Due to thermal expansion, therefore, the hot mantle is always less dense than the cooler lithosphere. It would be simple to separate surface plates and mantle into two domains with distinct material properties. The "thermal buoyancy number" ($\rho_0 g \alpha$) of each domain could then be manipulated independently to produce desired density contrasts between surface lithosphere and underlying mantle. The properties of the subducting slab, however, are more difficult to isolate from the surrounding mantle because ConMan operates in an Eulerian reference frame: material parameters are fixed relative to the grid; they do not move with the fluid.

Development of flexible, self-consistent, numerical viscous flow models is uniquely valuable to studies of Earth's retreating subduction systems. Geological and geophysical observations suggest the density of downgoing lithosphere is fundamentally related to rates of trench migration. Theoretical modeling is designed to complement and guide this observational research by providing a medium through which to explore and quantify the influence of slab density on subduction rate, mantle flow, and slab geometry. Moreover, models that realistically simulate subduction of compositionally variable lithosphere (containing both oceanic and continental materials) can provide insight not only into the effects of slab density on subduction dynamics but into the length and time scales over which these effects occur.

REFERENCES

Chen, J., and S. D. King (1998), The influence of temperature and depth dependent viscosity on geoid and topography profiles from models of mantle convection, *Physics of the Earth and Planetary Interiors, 106*, 75-92.

Conrad, C. P., and B. H. Hager (2001), Mantle convection with strong subduction zones, *Geophysics Journal International, 144*, 271-288.

Enns, A., T. W. Becker, and H. Schmeling, The dynamics of subduction and trench migration for viscosity stratification, in preparation for *Geophysics Journal International*, http://www/igpp.ucsd.edu/~tbecker/preprints/ebs03.pdf.

Faccenna, C., T. W. Becker, F. P. Lucente, L. Jolivet, and F. Rossetti (2001), History of subduction and back-arc extension in the Central Mediterranean, *Geophysics Journal International, 145*, 809-820.

Funiciello, F., G. Morra, K. Regenauer-Lieb, and D. Giardini (2003), Dynamics of retreating slabs: 1. Insights from two-dimensional numerical experiments, *Journal of Geophysical Research, 108*(B4), 2206, doi:10.1029/2001JB000898.

Kahle, H., M. V. Müller, A. Geiger, G. Danuser, S. Mueller, G. Veis, H. Billiris, and D. Paradissis (1995), The strain field in northwestern Greece and the Ionian Islands: results inferred from GPS measurements, *Tectonophysics, 249*, 41-52.

Kincaid, C., and R. W. Griffiths (2003), Laboratory models of the thermal evolution of the mantle during rollback subduction, *Nature, 425*, 58-62.

Le Pichon, X. (1982), Land-locked oceanic basins and continental collision: the Eastern Mediterranean as a case example, in *Mountain Building Processes*, edited by K. J. Hsue, pp. 201-211, Academic Press, San Diego, California.

McKenzie, D. (1972), Active tectonics of the Mediterranean region, *Geophysics Journal of the Royal Astronomical Society, 30*, 109-185.

Royden, L. H. (1993a), The tectonic expression of slab pull at continental convergent boundaries, *Tectonics, 12*, 303-325.

Royden, L. H. (1993b), Evolution of retreating subduction boundaries formed during continental collision, *Tectonics*, 12, 629-638.

Royden, L., and B. C. Burchfiel (1989), Are systematic variations in thrust belt style related to plate boundary processes? (The Western Alps versus the Carpathians), *Tectonics, 8*, 51-61.

Royden, L. H., S. A. Bowring, C. B. Burchfiel, S. Rondenay, and B. P. Weiss, Collaborative research: multi-disciplinary experiments for dynamic understanding of subduction under the Agean Sea (MEDUSA), Proposal to the National Science Foundation, submitted December, 2003.

Turcotte, D. L., and G. Schubert (2002), *Geodynamics*, 2nd ed., 456 pp., Cambridge University Press, New York.